



# HHS Public Access

Author manuscript

Cell Rep. Author manuscript; available in PMC 2016 August 18.

Published in final edited form as:

Cell Rep. 2015 August 18; 12(7): 1071–1079. doi:10.1016/j.celrep.2015.07.008.

## Metabolic Damage and Premature Thymus Aging Caused by Stromal Catalase Deficiency

Ann V Griffith<sup>1,5</sup>, Thomas Venables<sup>1</sup>, Jianjun Shi<sup>1</sup>, Andrew Farr<sup>2</sup>, Holly van Remmen<sup>3</sup>, Luke Szweda<sup>3</sup>, Mohammad Fallahi<sup>1</sup>, Peter Rabinovitch<sup>4</sup>, and Howard T. Petrie<sup>1,\*</sup>

<sup>1</sup>Department of Immunology and Microbial Sciences, The Scripps Research Institute, 130 Scripps Way, Jupiter, FL 33458, USA

<sup>2</sup>Departments of Biological Structure and Immunology, The University of Washington, South Lake Union E-411, 750 Republican Street, Box 358059, Seattle, WA 98109, USA

<sup>3</sup>Free Radical Biology and Aging Research Program, The Oklahoma Medical Research Foundation, MS 21, 825 NE 13<sup>th</sup> Street, Oklahoma City, OK 73104, USA

<sup>4</sup>Department of Pathology, The University of Washington, 1959 NE Pacific Avenue, HSB K-081, Box 357705, Seattle, WA 98195, USA

### SUMMARY

T lymphocytes are essential mediators of immunity that are produced by the thymus in proportion to its size. The thymus atrophies rapidly with age, resulting in progressive diminution of new T cell production. This decreased output is compensated by duplication of existing T cells, but it results in gradual dominance by memory T cells and decreased ability to respond to new pathogens or vaccines. Here, we show that accelerated and irreversible thymic atrophy results from stromal deficiency in the reducing enzyme catalase, leading to increased damage by hydrogen peroxide generated by aerobic metabolism. Genetic complementation of catalase in stromal cells diminished atrophy, as did chemical antioxidants, thus providing a mechanistic link between antioxidants, metabolism, and normal immune function. We propose that irreversible thymic atrophy represents a conventional aging process that is accelerated by stromal catalase deficiency in the context of an intensely anabolic (lymphoid) environment.

---

This is an open access article under the CC BY-NC-ND license (<http://creativecommons.org/licenses/by-nc-nd/4.0/>).

\*Correspondence: [hpetrie@scripps.edu](mailto:hpetrie@scripps.edu).

<sup>5</sup>Present address: Department of Microbiology and Immunology, School of Medicine, University of Texas Health Science Center at San Antonio, 7703 Floyd Curl Drive-MC 7758, San Antonio, TX 78229, USA

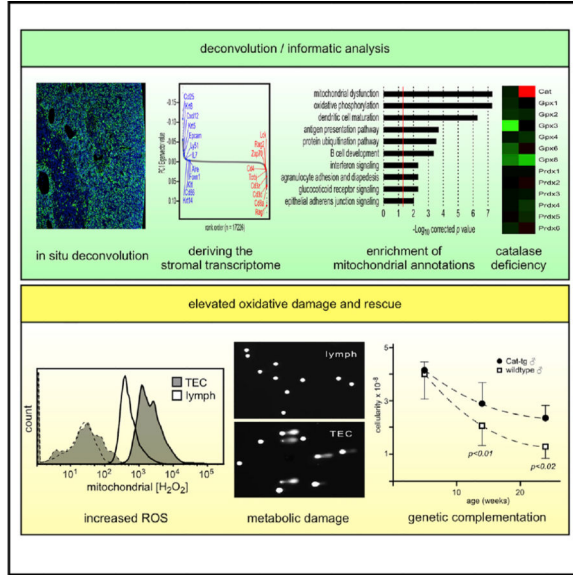
### SUPPLEMENTAL INFORMATION

Supplemental Information includes Supplemental Experimental Procedures and one figure and can be found with this article online at <http://dx.doi.org/10.1016/j.celrep.2015.07.008>.

### AUTHOR CONTRIBUTIONS

A.V.G. performed most of the wet-laboratory experiments and commented on the manuscript before submission. T.V. performed the informatic analysis and commented on the manuscript before submission. J.S. performed some wet-laboratory experiments and commented on the manuscript before submission. A.F. performed some wet-laboratory experiments and commented on the manuscript before submission. H.v.R. provided HPLC results and commented on the manuscript before submission. L.S. supplied unique reagents and commented on the manuscript before submission. M.F. contributed to developing informatics methods/tools and commented on the manuscript before submission. P.R. supplied unique reagents and commented on the manuscript before submission. H.T.P. supervised the experiments and informatic analysis, performed some wet-laboratory experiments, and wrote the manuscript.

### Graphical Abstract



### INTRODUCTION

T lymphocytes, like all hematopoietic cells, are continuously lost and must be replaced throughout life by the thymus. Developing lymphocytes are present in the thymus only transiently, and the durable identity of the thymus is thus established by its stable (stromal) components, consisting mainly of epithelial cells with lesser contribution by mesenchymal, myeloid, neuronal, and vascular cells (reviewed in Petrie and Zúñiga-Pflücker, 2007). Stromal cells provide most of the signals for T lineage differentiation (Petrie and Zúñiga-Pflücker, 2007) and regulate lymphoid cellularity by providing limited numbers of niches for lymphopoietic progenitors (Prockop and Petrie, 2004). Consequently, the integrity of thymic stroma is critical for the maintenance of thymic function.

The thymus reaches maximum size around the time of puberty, followed by rapid, progressive atrophy (reviewed in Montecino-Rodriguez et al., 2005). Since T cell production is proportional to thymic mass (Haynes et al., 2000), age-related atrophy results in progressive diminution of new T production by the thymus (Hale et al., 2006). While frank lymphopenia is masked by the ability of peripheral T lymphocytes to duplicate themselves (Surh and Sprent, 2008), the end result is a gradual drift toward immunologic memory, especially representing latent or persistent viral infections (Nikolich-Zugich and Rudd, 2010). In contrast, response to new antigens becomes progressively more limited, resulting in well-recognized consequences for the aging population.

The biological pressure and mechanisms of accelerated thymic atrophy remain unclear, although we have recently shown that it is primarily a stromal effect (Griffith et al., 2012) that results in fewer lymphoid cells via the niche effect described above. Sensitivity to sex steroids, especially androgens, remains the most popular theory for stromal atrophy, based on compelling but nonetheless correlative findings, including maximum size prior to puberty

(Domínguez-Gerpe and Rey-Méndez, 2003), increased atrophy in males (Aspinall and Andrew, 2001), and reduced atrophy when androgen response is impaired (Olsen et al., 2001) or ablated (Henderson, 1904). Castration also induces robust regeneration of the atrophied thymus (Utsuyama and Hirokawa, 1989; Goodall, 1905; Sutherland et al., 2005). However, such regrowth is transient even though androgen reduction is permanent (Griffith et al., 2012). Thus, while the thymus is exquisitely responsive to sex steroids, they cannot explain irreversible age-related atrophy of the thymus or why it is so dramatically accelerated compared with other tissues.

Among obstacles to working with stromal cells are that they are rare (<0.1% of thymic cellularity), difficult to isolate (because of formation of tight junctions and desmosomes), and most importantly, change dramatically upon removal from their native context, including downregulation of Notch ligands that are critical for T cell development (Mohtashami and Zúñiga-Pflücker, 2006). Several years ago, we devised a computational approach for in situ deconvolution of stromal gene signatures from thymic tissue (Griffith et al., 2009; Gosink et al., 2007), eliminating the need to isolate them. In those studies, we noted that the global transcriptome of stromal cells was unexpectedly enriched in processes associated with metabolism. Here, we show that a completely independent non-presumptive approach reinforces this conclusion, with specific emphasis on mitochondrial metabolism and mitochondrial dysfunction. We show that these annotations arise because epithelial stromal cells of the thymus are deficient in the enzyme catalase, leading to elevated stromal damage by reactive oxygen species (ROS). Our findings show that the acceleration of age-associated atrophy in the thymus is a consequence of inherent deficiency of catalase in stromal cells, leading to oxidative damage in the context of a highly metabolic environment designed to support the demands of lymphoblastic proliferation.

## RESULTS

### Deconvolution Analysis of Stromal versus Lymphoid Gene Profiles In Situ

Our original approach (Griffith et al., 2009) utilized ratiometric subtraction of gene expression in purified lymphoid cells versus the corresponding (microdissected) tissue to derive stromal gene signatures. Since then we have continued to experiment with other approaches for improved discrimination of stromal versus lymphoid transcriptomes in whole tissue. We first improved statistical accuracy in our publicly available data (GEO: GSE18281) by selecting the five arrays for each sample type with the best MAS5 scaling factors (<http://www.bioconductor.org/packages/release/bioc/html/affy.html>). We defined genes receiving at least three Present detection calls (MAS5) in each sample type, OR having a (gcRMA) signal greater than the chip median in at least three cases in each sample type, as being expressed in that tissue (29,206 probesets, representing 14,389 genes). We used the average gcRMA signal from purified lymphoid cells from either compartment, together with a calculated lymphoid proportion for each compartment (Griffith et al., 2009), to generate a calculated stromal signal for each probeset/gene on each tissue gene chip. We then used the LIMMA package (Gentleman et al., 2004) in R to identify 17,226 probesets (representing 10,427 genes) that were differentially expressed (LIMMA  $p < 0.05$  and gcRMA fold change  $\geq 2$ ) between tissue types. Principle component analysis (prcomp in R,

with gene centering, without variance scaling) was then used for dimensional reduction of the data (Figure 1A). Mapping a manually curated list of well-recognized genes for each sample type (Figures 1B–1E) revealed that the first principle component (PC1), accounting for nearly half of the total variance between samples, effectively projected differences between stromal and lymphoid cells. In contrast, PC2 was not efficient at distinguishing lymphoid versus stromal genes, but instead represented differences that distinguished cortical from medullary tissue (attributes that were not, in turn, projected by PC1). These outcomes show that the weights projected in PC1 can be used to effectively distinguish stromal signatures from composite thymic tissues.

### Catalase Deficiency in Stromal Cells

Understanding stromal biology has been plagued by a number of obstacles, as outlined in the Introduction. Our deconvolved stromal data provided a rich resource to address this deficiency. We used pathway analysis (Ingenuity) to characterize the biological networks highly associated with stromal-weighted genes derived from PC1 (Figure 1). As shown in Figure 2A, the two most significant pathways (corrected  $p < 10^{-7}$ ) were both associated with mitochondria, specifically mitochondrial dysfunction, and oxidative phosphorylation. Since ROS produced by mitochondria are thought to be key mediators in aging and since the thymus is arguably the fastest aging tissue in the body, we contemplated whether these associations might provide novel mechanistic insights into thymic age atrophy. Manually examining the genes associated with these enriched functions revealed that thymic stromal cells, especially cortical cells representing the component most profoundly affected by aging (Griffith et al., 2012), were deficient in the  $H_2O_2$ -reducing enzyme catalase (Figures 2B and 2C). Dramatic differences in catalase levels between cell types are not unexpected because catalase is in the top 4% most variable genes among body tissues in both humans (Figure 2D) and mice (Figure 2E) using publicly available data (Wu et al., 2009). Because of its extreme catalytic rate ( $>4 \times 10^7$   $H_2O_2$  molecules per second), low catalase levels would be expected to have a profound effect when ROS levels are high, as is likely to be found in the intensely anabolic environment supporting lymphoblastic proliferation in the thymus, where a substantial proportion of cells labels with a DNA analog in a short 4-hr pulse (Penit, 1988; Lind et al., 2001). Thus, stromal catalase deficiency, in the context of prolonged exposure to high-level ROS, represented a potential mechanism to explain accelerated thymic atrophy.

In order to further validate our deconvolution approach using stromal cells isolated in a more conventional manner, we used publicly available data (Ki et al., 2014) and a web-based normalization algorithm (GExC) based on approximately 12,000 diverse data sets (Seita et al., 2012). Analysis of catalase gene expression in these data (Figure S1) confirmed that while thymic lymphoid cells are relatively high in catalase expression and would thus be protected from peroxide damage, purified cortical thymic epithelial cells (cTEC) or medullary thymic epithelial cells (mTEC) were both relatively deficient in catalase. These independent data corroborated our findings using a conventional approach to stromal characterization, further substantiating the potential of catalase deficiency as a mechanism for accelerated age atrophy of the thymus.

## Biochemical or Genetic Enhancement of Antioxidant Activity Inhibits Thymic Atrophy

To determine whether mitochondrial dysfunction and catalase deficiency played a role in accelerated thymic atrophy, we implemented two distinct but complementary approaches. First, mice were given literature-consensus doses of two common antioxidants (n-acetylcysteine or L-ascorbate) in drinking water from the time of weaning, and thymic size was measured at 10 weeks (Figure 3A), at which point thymuses from WT mice had lost approximately 40% of their size. Despite no efforts to optimize antioxidant dose, thymuses from antioxidant-supplemented mice were significantly larger than controls ( $p < 0.002$ ), with n-acetylcysteine almost eliminating atrophy in supplemented mice. Other body tissues were not affected by supplementation (Figure 3B), indicating the absence of any adverse effects of supplementation.

Given this strong supporting evidence for the hypothesis that oxidative damage resulting from catalase deficiency might explain accelerated thymic atrophy with age, we specifically focused on the role of catalase using a transgenic mouse where mitochondrially targeted catalase was ubiquitously expressed (Schriner et al., 2005). Cellularity in transgenic mice versus control littermates was indistinguishable in young mice (5 weeks of age); this is not surprising since metabolic damage accumulates over time and since this age represents peak size in WT mice and therefore precedes the onset of metabolic damage. At later time points, however, organ size was substantially elevated in the presence of the transgene, such that thymus size in 6-month-old transgenic mice was more than double that of age-matched controls or about the same size as in controls at 10 weeks of age (Figure 3C). While we used male mice in most of our experiments because atrophy is more pronounced in males than in females (due to androgen responsiveness that is independent of irreversible age-related atrophy, even though both affect thymus size; see Discussion), genetic supplementation of catalase revealed similar protective effects on thymus size in female mice (Figure 3D), confirming that this effect is not directly linked to androgen levels.

These studies provided strong evidence that thymic atrophy is impacted by redox state. However, in both cases, antioxidant effects were present in both stromal and lymphoid cells in the thymus. To directly link these effects to thymic stromal cells, we performed classical reciprocal bone marrow transplant experiments, transferring WT or Cat-tg lineage-negative marrow into WT or Cat-tg recipients. In all cases, recipient mice were also deficient in *Il7ra*, allowing hematopoietic reconstitution of the recipient thymus without the need for myeloablation (Prockop and Petrie, 2004), which has its own effects on cellularity. Cat-tg effects mapped exclusively to the recipient (i.e., non-transplantable stromal cells) and were independent of the donor (lymphoid) cells (Figure 3E). Thus, genetic complementation of catalase exclusively in thymic stromal cells was sufficient to mitigate its protective effects and ameliorate rapid thymic atrophy with age.

## Thymic Stromal Cells Exhibit Elevated Levels of the Hallmarks of Oxidative Damage

The hypothesis that genetic complementation of catalase in stromal cells would confer resistance to atrophy (Figure 3) also predicts that unprotected thymic stromal cells would exhibit elevated levels of lesions associated with ROS. To test this, we measured two classical types of oxidative damage to DNA. In the first, we used high-performance liquid

chromatography (HPLC) to measure the presence of 8-hydroxy-2-deoxyguanosine (8OHdG), a common product of 2-deoxyguanosine (2dG) oxidation, in DNA isolated from stromal cells or lymphoid cells derived from the same tissue (Figure 4A). To generate enough sample for HPLC, given the limiting numbers of stromal cells, we used a simple enrichment procedure involving repeated cycles of gentle physical liberation of lymphoid cells from thymic tissue, followed by unit gravity sedimentation of enriched stromal rudiments. Even though histological examination of such tissue indicated that it still consisted of >50% lymphoid cells (not shown), a sizeable 3- to 4-fold increase in 8OHdG levels was seen.

To further substantiate these findings in isolated stromal cells, we used single-cell gel electrophoresis (SCGE) to measure DNA (chromatin) unwinding that is induced by various forms of oxidative DNA damage. This assay, also known as the “comet” assay (Ostling and Johanson, 1984) because of its characteristic appearance (Figure 4C), allows quantitative assessment of both the proportion of damaged cells (cells with or without tails), as well as the severity of damage in each cell (percentage of total cellular DNA in tail, length of tail). In these purified cell assays, we focused on TEC, the predominant stromal cell type in the thymus (for an example, see Klug et al., 1998). To unambiguously define TEC even after extensive tissue digestion, we used mice carrying a Cre allele knocked in to the *Foxn1* locus (Gordon et al., 2007) to activate a conditional (*Rosa26*-driven) fluorescent reporter in a lineage-specific manner. Lymphoid cells (identified as being CD45<sup>+</sup>) and TEC were then simultaneously purified from the same sample by cell sorting, followed by SCGE. TEC exhibited a much greater frequency of cells with tails than did lymphoid cells from the same sample (Figure 4D), and the percent of DNA in the tail, as well as tail length, was also greater, substantiating the finding that TEC contains elevated levels of lesions consistent with oxidative damage. While we used paired thymic lymphoid cells as controls here, we also tested epithelial cells from other tissues, but in all cases, we observed more damage in these other epithelial cells than in TEC. We believe this reflects the more aggressive mechanical and enzymatic methods required to liberate epithelial cells from these stratified and tightly joined epithelial tissues. However, it is also possible that catalase levels are even lower in epithelial cells from these tissues. In any case, increased damage makes them unsuitable as controls for evaluating damage in TEC, while thymic lymphoid cells, isolated and analyzed side by side with TEC, represent a perfectly paired control, especially since only viable (DAPI<sup>-</sup>) cells were analyzed in both cases.

### **Epithelial Stromal Cells Accumulate More H<sub>2</sub>O<sub>2</sub> and Are More Sensitive to H<sub>2</sub>O<sub>2</sub> Damage Than Their Lymphoid Counterparts in the Thymus**

Our findings thus far indicate that TEC are deficient in catalase and thus rapidly accumulate lesions consistent with oxidative metabolic damage. To directly establish a relationship between the catalase substrate H<sub>2</sub>O<sub>2</sub> and thymic stromal cells, we performed two different types of experiments. First, we used the fluorescent chemical probe MitoPy1 (Tocris Biosciences) to directly measure H<sub>2</sub>O<sub>2</sub> levels in mitochondria from TEC or lymphoid cells in the same biological sample (distinguished by gating as described in the preceding section). The results of this highly specific assay show that TEC exhibit higher levels of mitochondrial H<sub>2</sub>O<sub>2</sub> than paired lymphoid cells (approximately one log<sub>10</sub> level of

fluorescence, Figure 5A), consistent with decreased catalase activity. We then directly challenged freshly isolated cell suspensions directly with 500  $\mu\text{M}$   $\text{H}_2\text{O}_2$  and measured mitochondrial membrane potential (DiIC1 staining) as an indicator of mitochondrial integrity. Even prior to  $\text{H}_2\text{O}_2$  treatment (directly ex vivo), freshly isolated TEC exhibited lower membrane potential than paired lymphoid cells from the same thymus (Figure 5B), consistent with higher levels of pre-existing damage. Treatment with  $\text{H}_2\text{O}_2$  resulted in a further decrease in mitochondrial membrane potential in TEC, while lymphoid cells from the same sample were barely affected by this treatment. These results further confirm that TEC exhibit high concentrations of the catalase substrate  $\text{H}_2\text{O}_2$ , as well as elevated sensitivity to  $\text{H}_2\text{O}_2$ , both of which are further characteristic of decreased activity of the reducing enzyme catalase.

## DISCUSSION

Lymphocytes are unique among body tissues in that their defining function is not germline encoded, but rather derives from permutational recombination of variable gene segments in somatic cells. The result is enormous diversity (estimated at  $>2.5 \times 10^7$  specificities) without the need for a proportional genetic burden. However, since each T has a unique receptor recognizing essentially one specific peptide antigen, panoramic immunity depends on the continuous production of large numbers of cells, each with a different receptor. This production is the function of the thymus, which manufactures cells in direct proportion to its mass (Haynes et al., 2000). The mass of the thymus, in turn, is regulated by the size and integrity of its stromal compartment, which restricts the size of the lymphoid pool by providing limited numbers of competitive niches for early lymphopoietic progenitors (Prockop and Petrie, 2004). Thus, stromal health is essential for thymus size and thus for the continuous production of a broad diversity of antigen specific T cells.

Enigmatically, the thymus reaches absolute peak size at around adolescence, declining rapidly and progressively thereafter with age (Domínguez-Gerpe and Rey-Méndez, 2003). Thus, the production of new T cells, with their diverse specificities, also decreases rapidly and progressively with age. This loss of diversity is obscured by the homeostatic expansion of peripheral T cells (Surh and Sprent, 2008), thereby preventing the appearance of frank lymphopenia, but each instance of antigen or pathogen exposure consists of selective clonal expansion followed by non-selective loss of all T cells in the return to homeostasis. Consequently, the peripheral T cell pool loses diversity in the absence of new T cell production, gradually becoming more biased toward past exposure (immunologic memory), while forward-looking, broad-spectrum immunity is diminished. Aging is therefore associated with diminution of the ability to respond to new immunologic challenges, including both evolving pathogens and the vaccines that may otherwise offer protection from them.

Early atrophy of the thymus is primarily a stromal function (Griffith et al., 2012), but because of limitations in isolation of pristine stromal cells (as discussed earlier), the pathological mechanisms underlying stromal (and therefore thymic) atrophy have been difficult to define. The prevailing theory invokes stromal sensitivity to sex steroids, based on a number of very reasonable but correlative observations (see Introduction). It is important

to stress that there is absolutely no question that the thymus is exquisitely responsive to sex steroids, especially androgens; in fact, it is inarguably (and perhaps inexplicably) one of the most androgen-responsive tissues in the body. There is also no question that thymus cellularity is inversely correlated with sex steroid levels. However, we believe it is essential to make the distinction between the effects of sex steroids on thymus cellularity and the effects of the aging process on thymus cellularity. A key distinction is the demonstration that castration-induced regrowth of the aged thymus is a transient response, with a return to the original (atrophied) state in within 2 weeks in mice (Griffith et al., 2009); since androgen levels do not re-equilibrate, the castration response and the underlying state of atrophy are not linked. Independence of hormonal influences and age atrophy can also be seen in studies of wild animals (Kendall, 1981), where thymus size oscillates with seasonal (hormonal) influences while trending ever smaller over the long term. Further, the initiation of thymic atrophy in humans may occur as early as neonatally (Steinmann et al., 1985) and certainly is present long before puberty. Finally, and somewhat more anecdotally, aging as a consequence of androgen exposure is at odds with the decrease in androgens that occurs with age, as well as with the popularity of androgen therapy as a mechanism to “reverse” aging.

Our studies show that rather than an idiosyncratic relationship to sex steroids, thymic atrophy represents the widely recognized process of accumulated macromolecular damage, resulting from lifelong exposure to the oxidative byproducts of aerobic metabolism. Atrophy resulting from accumulated damage is documented in many organs and tissues as part of the “normal” aging process (He et al., 2009) and is intimately linked to aerobic metabolism and oxygen radicals. However, these are generally slow, progressive processes that do not become apparent until late in life and, with the notable exception of skeletal muscle, often go mostly unnoticed. In the case of the thymus, atrophy is more rapid than other tissues, which we now show is a consequence of stromal catalase deficiency, resulting in accelerated stromal damage and tissue atrophy. It is worth noting that much like elevation of antioxidant activity, downmodulation of metabolic activity, either by caloric restriction (Yang et al., 2009) or by decreased bioavailability of Igf (Vallejo et al., 2009), also impairs thymic atrophy, further strengthening the link between thymic atrophy and metabolic damage.

Finally, we note that while reconstitution of catalase in stromal cells reduces atrophy, it does not abolish it. It is possible that the mitochondrially targeted catalase transgene is not optimal since  $H_2O_2$  is also produced in substantial quantity by peroxisomes. However, neither endogenous nor transgenic catalase completely prevents metabolic damage, in the thymus or any other tissue, and aging (and atrophy) thus continues, albeit at a slower rate, regardless of antioxidant levels or other modulation of metabolic activity.

## EXPERIMENTAL PROCEDURES

### Identification of Global Stromal or Lymphoid Gene Expression Profiles

We modified our previously described approach for deriving stromal gene signatures in situ (Griffith et al., 2009). A subset of the data made public in association with that manuscript (GEO: GSE18281) was used. For each tissue type (cortical, medullary, lymphoid, tissue), the five gene chips with the lowest scaling factors were chosen. Genes defined as being

expressed in cortical or medullary tissue were identified as the union of genes receiving at least 3/5 Present detection calls (Affymetrix MAS5 algorithm) or having a gcRMA signal greater than the median in 3/5 gene chips. We then used the five-chip average signal derived from lymphoid cells from either compartment with a calculated lymphoid proportion for each compartment (Griffith et al., 2009) to generate a calculated stromal signal for each probeset/gene on each tissue gene chip. We then used LIMMA (Gentleman et al., 2004) in R to identify 17,226 probesets (10,427 genes) that were differentially expressed between these tissue types (unadjusted LIMMA  $p < 0.05$  and fold change  $\geq 2$ ). Principle component analysis (prcomp in R, with gene centering, without variance scaling) was performed for dimension reduction. Gene lists derived from principle components (e.g., the top or bottom 5% of genes in PC1, for Figure 1) were analyzed using Ingenuity Pathway Analysis software (<http://www.qiagen.com>) for pathway enrichment using default parameters.

### Body Atlas Data

Complete MOE430 (mouse) and U133 (human) microarray tissue atlas data sets (Wu et al., 2009) were downloaded from the repository (<http://www.biogps.org>). Probeset to gene mapping was done using mouse4302.db and hgu133plus2.db packages in R. Multiple probesets were collapsed to a single gene using the collapseRows() function from the R WGCNA package. Tissue gene variance was measured with the rowVars() function in R. The resulting variances were rank ordered and plotted.

### Mice

All experimental mice were on the C57BL/6 background. Foxn1<sup>tm3(cre)Nrm</sup> mice (stock #018448), Gt(ROSA)26Sor<sup>tm1(EYFP)Cos</sup> mice (stock #006148), and B6.129S7-II7r<sup>tm1Imx</sup> mice (stock #002295) were obtained from Jackson Laboratories. Conditional Rosa26[tdRFP] mice (Luche et al., 2007) and mCat-transgenic mice (Schriner et al., 2005) were obtained from the originating laboratories. All strains and crosses were bred and maintained at Scripps-Florida. All animal use was approved by an institutional animal care and use committee.

### Stromal Isolation

For large-scale isolation of enriched stromal cells for HPLC, thymuses were minced into fine pieces followed by gentle but thorough rolling between two glass slides. The stromal remnants were allowed to settle by unit gravity, and lymphoid cells were derived from the suspension. All steps were performed on ice. For purification of genetically marked thymic epithelial cells, Foxn1<sup>tm3(cre)Nrm</sup> mice were crossed with Gt(ROSA) 26S or<sup>tm1(EYFP)Cos</sup> mice, resulting in expression of EYFP in all thymic epithelial cells, or with similar mice using an RFP reporter (Luche et al., 2007), depending on the fluorochromes required downstream. Thymuses were harvested and carefully minced with a scalpel. Fragments were passed multiple times through a pipet, and large pieces were allowed to settle, followed by removal of most of the supernatant (lymphoid cells). Remaining fragments were then subjected to digestion with collagenase (0.125%) for 10 min at 37°C. Pipetting, sedimentation, removal of lymphoid cells were repeated three additional times, followed by a final digestion in trypsin (0.05%). After the final digestion, all cells (lymphoid and

stromal) were washed, pelleted by centrifugation, and resuspended and stained with a fluorescent antibody recognizing CD45 (Ly-5). Epithelial cells and lymphoid cells were then separated by cell sorting at low pressure using a 100  $\mu\text{m}$  nozzle. Dead and/or dying cells were excluded by staining with DAPI.

### Measurement of Oxidative DNA Damage by HPLC

The levels of 8OHdG were determined as previously described (Hamilton et al., 2001). Nuclear DNA was isolated with a DNA Extractor WB kit (catalog # 291–50502; Waco Chemicals), which implements NaI, rather than phenol, to minimize exogenous oxidation (Hamilton et al., 2001). Nucleotides were liberated by incubation with nuclease P1 and alkaline phosphatase. The levels of 8OHdG or 2-dG in the deoxynucleoside mixture were measured by HPLC with electrochemical and UV detection (Model 5200; ESA) using a reverse-phase Supelcosil LC-18-T column (Supelco). A 25 mM sodium acetate (pH 5.0–5.2) containing 5% methanol was used as mobile phase in the isocratic system. 8OHdG and 2dG were expressed as the ratio of nmol of 8OHdG per  $10^5$  nmol of 2-dG.

### Comet Assay

The alkaline comet assay was carried out using a kit from Trevigen (#4250-050-K) per the manufacturer's recommendations. Sorted TEC or an equivalent number of thymic lymphoid cells sorted in parallel was washed once in Hank's balanced salt solution (HBSS), followed by resuspension of the pellet in 50  $\mu\text{l}$  of low melting temperature agarose, and then analyzed after electrophoresis and staining with Sybr Green. Images were acquired using an Olympus BX-50 fluorescent microscope. The proportion of damaged cells and the percentage of DNA in the tails of damaged cells were calculated using Open Comet software (Gyori et al., 2014).

### Supplementation with Dietary Antioxidants

At the time of weaning, mice were placed immediately onto pure water or water supplemented with N-acetylcysteine or L-ascorbate acid at 15 mg/ml. Water was prepared fresh twice weekly until the time of euthanasia. Estimated actual dosages for N-acetylcysteine or L-ascorbate were 2.6 and 2.7 g/kg/day, respectively. Prior to euthanasia, body composition (fat mass, lean mass) was assessed at 7.5 MHz using a Minispec LF50 Body Composition Analyzer (Bruker Optics).

### Reciprocal Bone Marrow Transplantation

Donor bone marrow was derived from young hemizygous mCat-Tg mice or WT littermate controls. CD3-negative bone marrow was prepared by cell sorting and transplanted by retro-orbital injection into non-irradiated  $\text{Il7ra}^{-/-}$  recipients, which were the offspring of [mCat-Tg<sup>+/-</sup>  $\text{Il7ra}^{-/-}$  X  $\text{Il7ra}^{-/-}$ ] crosses at 4–5 weeks of age. Thymic cellularity was determined approximately 10 weeks later by hemacytometer counting.

### Measurement of Mitochondrial $\text{H}_2\text{O}_2$

Enzymatically digested lympho-stromal preparations (described above) from (Fonxn1[Cre]  $\times$  reporter) mice were stained with an antibody recognizing CD45, and the entire preparation

was then stained for 20 min at 37°C using the fluorescent probe MitoPY1 (Tocris Biosciences, #4428) at a final concentration of 5 µM. Lymphoid cells (CD45<sup>+</sup>) and epithelial cells (reporter<sup>+</sup>) in the same sample were distinguished by electronic gating after acquisition. Dead cells were excluded by staining with DAPI.

### Analysis of Mitochondrial Integrity

Enzymatically digested lympho-stromal preparations (described above) from (Fonxn1[Cre] × reporter) mice were stained with an antibody recognizing CD45, and the entire preparation was stained for 15 min at 37°C with the cyanine dye DilC1 (1,1',3,3,3',3'-hexamethylindodicarbocyanine iodide, Life Technologies #M34151) at a final concentration of 0.3 nM. After washing, a portion of the sample was analyzed (untreated control), after which the remainder was treated with 500 µM H<sub>2</sub>O<sub>2</sub> at room temperature prior to reanalysis at 45 min (treated sample). Lymphoid cells (CD45<sup>+</sup>) and epithelial cells (reporter<sup>+</sup>) were distinguished by gating after acquisition.

### Supplementary Material

Refer to Web version on PubMed Central for supplementary material.

### Acknowledgments

This work was supported by PHS grants AG031576 and AI103340. We thank Laura Simo, Yangming Xiao, Richard Smith, and Ganesh Karunakaran for technical support; John Cleveland for suggesting antioxidant feeding experiments; Hans Joerg Fehling for RFP reporter mice; and Yousuke Takahama for insights into enzymatic digestion of thymic tissue.

### REFERENCES

- Aspinall R, Andrew D. Gender-related differences in the rates of age associated thymic atrophy. *Dev. Immunol.* 2001; 8:95–106. [PubMed: 11589313]
- Domínguez-Gerpe L, Rey-Méndez M. Evolution of the thymus size in response to physiological and random events throughout life. *Microsc. Res. Tech.* 2003; 62:464–476. [PubMed: 14635139]
- Gentleman RC, Carey VJ, Bates DM, Bolstad B, Dettling M, Dudoit S, Ellis B, Gautier L, Ge Y, Gentry J, et al. Bioconductor: open software development for computational biology and bioinformatics. *Genome Biol.* 2004; 5:R80. [PubMed: 15461798]
- Goodall A. The post-natal changes in the thymus of guinea-pigs, and the effect of castration on thymus structure. *J. Physiol.* 1905; 32:191–198. [PubMed: 16992768]
- Gordon J, Xiao S, Hughes B 3rd, Su DM, Navarre SP, Condie BG, Manley NR. Specific expression of lacZ and cre recombinase in fetal thymic epithelial cells by multiplex gene targeting at the Foxn1 locus. *BMC Dev. Biol.* 2007; 7:69. [PubMed: 17577402]
- Gosink MM, Petrie HT, Tsinoremas NF. Electronically subtracting expression patterns from a mixed cell population. *Bioinformatics.* 2007; 23:3328–3334. [PubMed: 17956877]
- Griffith AV, Fallahi M, Nakase H, Gosink M, Young B, Petrie HT. Spatial mapping of thymic stromal microenvironments reveals unique features influencing T lymphoid differentiation. *Immunity.* 2009; 31:999–1009. [PubMed: 20064453]
- Griffith AV, Fallahi M, Venables T, Petrie HT. Persistent degenerative changes in thymic organ function revealed by an inducible model of organ regrowth. *Aging Cell.* 2012; 11:169–177. [PubMed: 22103718]
- Gyori BM, Venkatachalam G, Thiagarajan PS, Hsu D, Clement MV. OpenComet: an automated tool for comet assay image analysis. *Redox Biol.* 2014; 2:457–465. [PubMed: 24624335]

- Hale JS, Boursalian TE, Turk GL, Fink PJ. Thymic output in aged mice. *Proc. Natl. Acad. Sci. USA*. 2006; 103:8447–8452. [PubMed: 16717190]
- Hamilton ML, Guo Z, Fuller CD, Van Remmen H, Ward WF, Austad SN, Troyer DA, Thompson I, Richardson A. A reliable assessment of 8-oxo-2-deoxyguanosine levels in nuclear and mitochondrial DNA using the sodium iodide method to isolate DNA. *Nucleic Acids Res*. 2001; 29:2117–2126. [PubMed: 11353081]
- Haynes BF, Sempowski GD, Wells AF, Hale LP. The human thymus during aging. *Immunol. Res*. 2000; 22:253–261. [PubMed: 11339360]
- He Q, Heshka S, Albu J, Boxt L, Krasnow N, Elia M, Gallagher D. Smaller organ mass with greater age, except for heart. *J. Appl. Physiol*. 2009; 106:1780–1784. [PubMed: 19325028]
- Henderson J. On the relationship of the thymus to the sexual organs: I. The influence of castration on the thymus. *J. Physiol*. 1904; 31:222–229. [PubMed: 16992746]
- Kendall, MD. Age and seasonal changes in the thymus. *The Thymus Gland, MD.*; Kendall, editors. London: Academic Press; 1981. p. 21-35.
- Ki S, Park D, Selden HJ, Seita J, Chung H, Kim J, Iyer VR, Ehrlich LI. Global transcriptional profiling reveals distinct functions of thymic stromal subsets and age-related changes during thymic involution. *Cell Rep*. 2014; 9:402–415. [PubMed: 25284794]
- Klug DB, Carter C, Crouch E, Roop D, Conti CJ, Richie ER. Interdependence of cortical thymic epithelial cell differentiation and T-lineage commitment. *Proc. Natl. Acad. Sci. USA*. 1998; 95:11822–11827. [PubMed: 9751749]
- Lind EF, Prockop SE, Porritt HE, Petrie HT. Mapping precursor movement through the postnatal thymus reveals specific microenvironments supporting defined stages of early lymphoid development. *J. Exp. Med*. 2001; 194:127–134. [PubMed: 11457887]
- Luche H, Weber O, Nageswara Rao T, Blum C, Fehling HJ. Faithful activation of an extra-bright red fluorescent protein in “knock-in” Cre-reporter mice ideally suited for lineage tracing studies. *Eur. J. Immunol*. 2007; 37:43–53. [PubMed: 17171761]
- Mohtashami M, Zúñiga-Pflücker JC. Three-dimensional architecture of the thymus is required to maintain delta-like expression necessary for inducing T cell development. *J. Immunol*. 2006; 176:730–734. [PubMed: 16393955]
- Montecino-Rodriguez E, Min H, Dorshkind K. Reevaluating current models of thymic involution. *Semin. Immunol*. 2005; 17:356–361. [PubMed: 15967677]
- Nikolich-Zugich J, Rudd BD. Immune memory and aging: an infinite or finite resource? *Curr. Opin. Immunol*. 2010; 22:535–540. [PubMed: 20674320]
- Olsen NJ, Olson G, Viselli SM, Gu X, Kovacs WJ. Androgen receptors in thymic epithelium modulate thymus size and thymocyte development. *Endocrinology*. 2001; 142:1278–1283. [PubMed: 11181545]
- Ostling O, Johanson KJ. Microelectrophoretic study of radiation-induced DNA damages in individual mammalian cells. *Biochem. Biophys. Res. Commun*. 1984; 123:291–298. [PubMed: 6477583]
- Penit C. Localization and phenotype of cycling and post-cycling murine thymocytes studied by simultaneous detection of bromodeoxyuridine and surface antigens. *J. Histochem. Cytochem*. 1988; 36:473–478. [PubMed: 2895787]
- Petrie HT, Zúñiga-Pflücker JC. Zoned out: functional mapping of stromal signaling microenvironments in the thymus. *Annu. Rev. Immunol*. 2007; 25:649–679. [PubMed: 17291187]
- Prockop SE, Petrie HT. Regulation of thymus size by competition for stromal niches among early T cell progenitors. *J. Immunol*. 2004; 173:1604–1611. [PubMed: 15265888]
- Schriner SE, Linford NJ, Martin GM, Treuting P, Ogburn CE, Emond M, Coskun PE, Ladiges W, Wolf N, Van Remmen H, et al. Extension of murine life span by overexpression of catalase targeted to mitochondria. *Science*. 2005; 308:1909–1911. [PubMed: 15879174]
- Seita J, Sahoo D, Rossi DJ, Bhattacharya D, Serwold T, Inlay MA, Ehrlich LI, Fathman JW, Dill DL, Weissman IL. Gene Expression Commons: an open platform for absolute gene expression profiling. *PLoS ONE*. 2012; 7:e40321. [PubMed: 22815738]
- Steinmann GG, Klaus B, Müller-Hermelink HK. The involution of the ageing human thymic epithelium is independent of puberty. A morphometric study. *Scand. J. Immunol*. 1985; 22:563–575. [PubMed: 4081647]

- Surh CD, Sprent J. Homeostasis of naive and memory T cells. *Immunity*. 2008; 29:848–862. [PubMed: 19100699]
- Sutherland JS, Goldberg GL, Hammett MV, Uldrich AP, Berzins SP, Heng TS, Blazar BR, Millar JL, Malin MA, Chidgey AP, Boyd RL. Activation of thymic regeneration in mice and humans following androgen blockade. *J. Immunol.* 2005; 175:2741–2753. [PubMed: 16081852]
- Utsuyama M, Hirokawa K. Hypertrophy of the thymus and restoration of immune functions in mice and rats by gonadectomy. *Mech. Ageing Dev.* 1989; 47:175–185. [PubMed: 2785623]
- Vallejo AN, Michel JJ, Bale LK, Lemster BH, Borghesi L, Conover CA. Resistance to age-dependent thymic atrophy in long-lived mice that are deficient in pregnancy-associated plasma protein A. *Proc. Natl. Acad. Sci. USA.* 2009; 106:11252–11257. [PubMed: 19549878]
- Wu C, Orozco C, Boyer J, Leglise M, Goodale J, Batalov S, Hodge CL, Haase J, Janes J, Huss JW 3rd, Su AI. BioGPS: an extensible and customizable portal for querying and organizing gene annotation resources. *Genome Biol.* 2009; 10:R130. [PubMed: 19919682]
- Yang H, Youm YH, Dixit VD. Inhibition of thymic adipogenesis by caloric restriction is coupled with reduction in age-related thymic involution. *J. Immunol.* 2009; 183:3040–3052. [PubMed: 19648267]

### Highlights

- The thymus exhibits accelerated atrophy with age due to changes in stromal cells
- Global transcriptome analysis reveals that stromal cells are deficient in catalase
- Stromal cells showed elevated H<sub>2</sub>O<sub>2</sub> levels and multiple hallmarks of oxidative damage
- Genetic or biochemical restoration of antioxidant activity ameliorates thymic atrophy

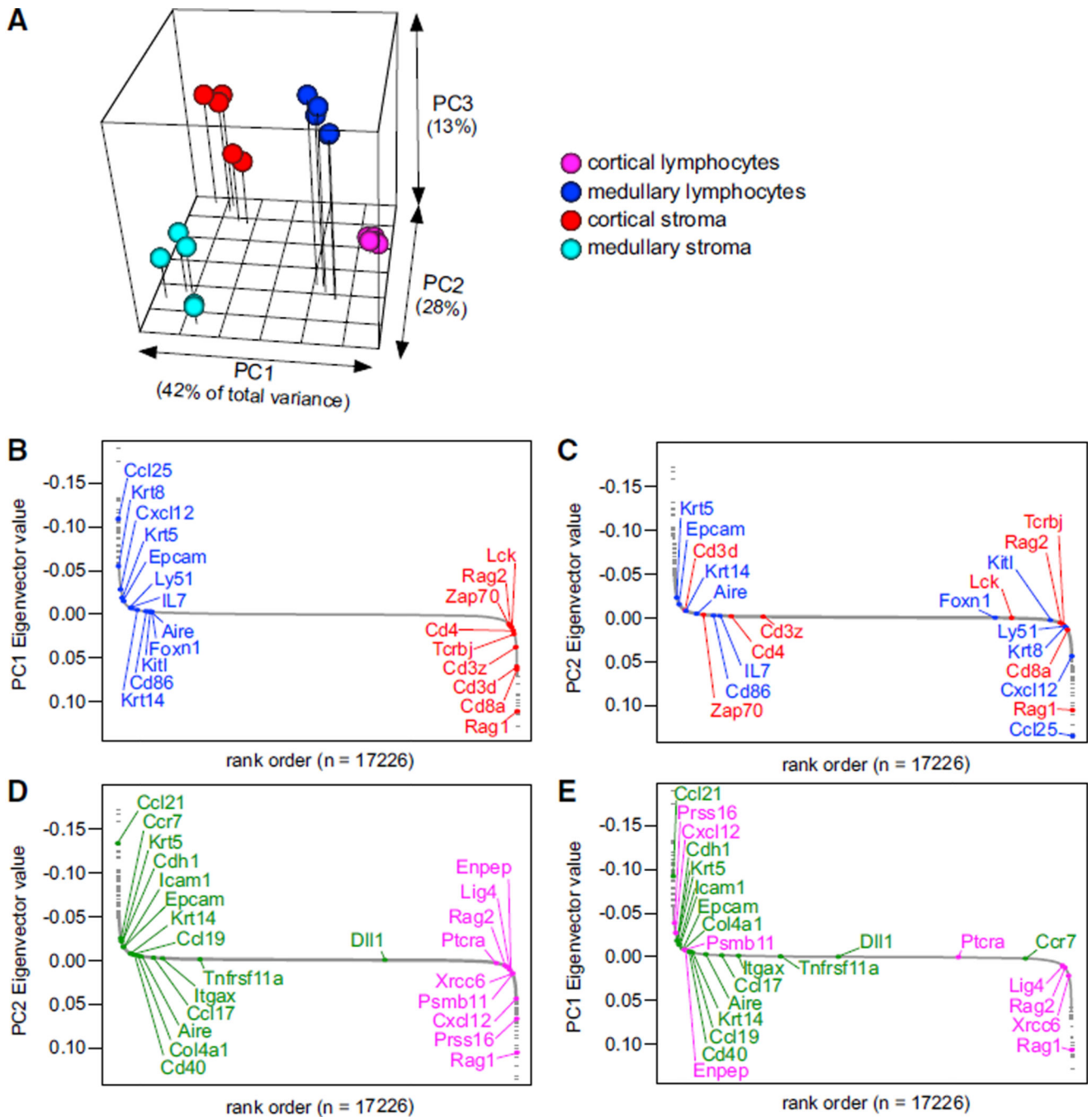


**Figure 1. Deconvolution and Principle Component Analysis of Stromal versus Lymphoid Gene Expression In Situ**

(A) Previously published data from our laboratory (contained in GEO dataset GEO: GSE18281) was processed and filtered as described in the text, followed by implementation of principle component analysis to distinguish the differences between samples. A dimensional view of the first three principle components is shown.

(B) The first principle component, accounting for a substantial proportion of the total variance (42%), accurately describes differences between lymphoid and stromal cells, as indicated by the distribution of lymphoid (red) versus stromal (blue) genes.

(C and D) In contrast, the next largest principle component (PC2, representing 28% of the sample variance), does not effectively separate lymphoid from stromal genes (C) and instead captures those genes that accurately distinguish cortical (magenta) from medullary (green) compartments (D).

(E) Similar to PC2 for lymphoid/stromal distinctions, PC1 performed poorly in distinguishing medullary versus cortical genes. This figure illustrates the utility of our current approach for stromal signal deconvolution and shows that the variances projected in PC1 can confidently be used to identify genes that characterize stromal (or lymphoid) cells in composite thymic tissues.

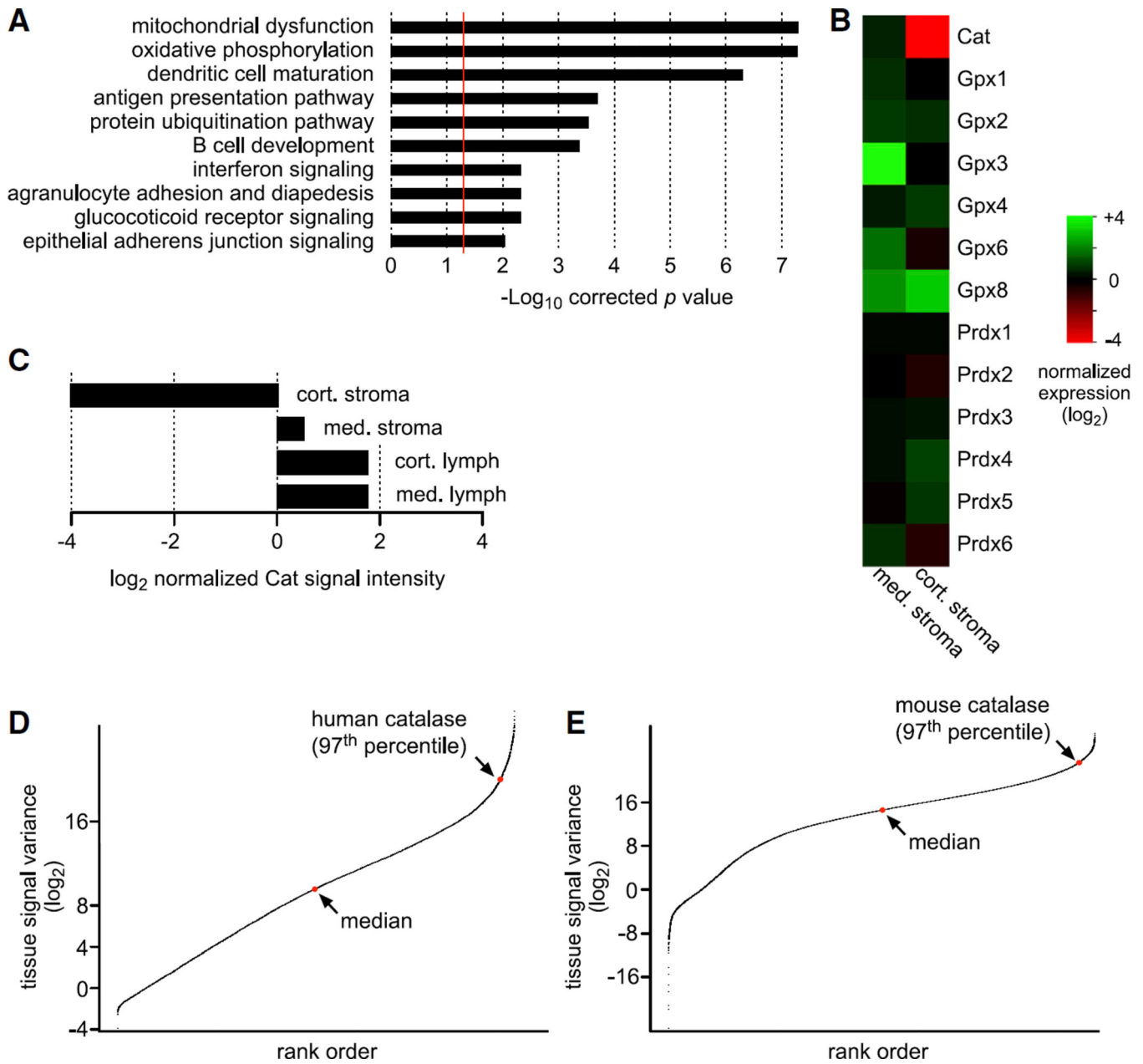


### Figure 2. Thymic Stromal Cells Are Deficient in Catalase

(A) Pathway analysis of the top 5% of stromal-weighted genes (PC1, Figure 1) revealed that metabolic processes, especially those involved in mitochondrial (dys)function or oxidative metabolism, were the most significant (only the top ten are shown; the red line indicates the threshold of significance, representing Benjamini-Hochberg corrected  $p < 0.05$ ).

(B) Relative expression of genes present in at least one tissue type (cortical or medullary), filtered on the ontology classification GO:0000302 (response to reactive oxygen species), indicating catalase deficiency in stromal cells, especially in the cortical compartment.

(C) Normalized gene expression shows that both cortical and medullary stroma were deficient in Cat compared with their corresponding lymphoid cells, with the most profound

deficiency in the cortex. Deconvolved stromal results are consistent with publicly available data on purified mTEC and cTEC (see Figure S1).

(D and E) Human and mouse body atlas data, respectively (multiple probesets collapsed to a single gene), indicating that catalase expression is in the 97<sup>th</sup> percentile of tissue variance in both cases and the differences in catalase levels between thymic stromal and lymphoid cells are not without precedent. See also Figure S1.

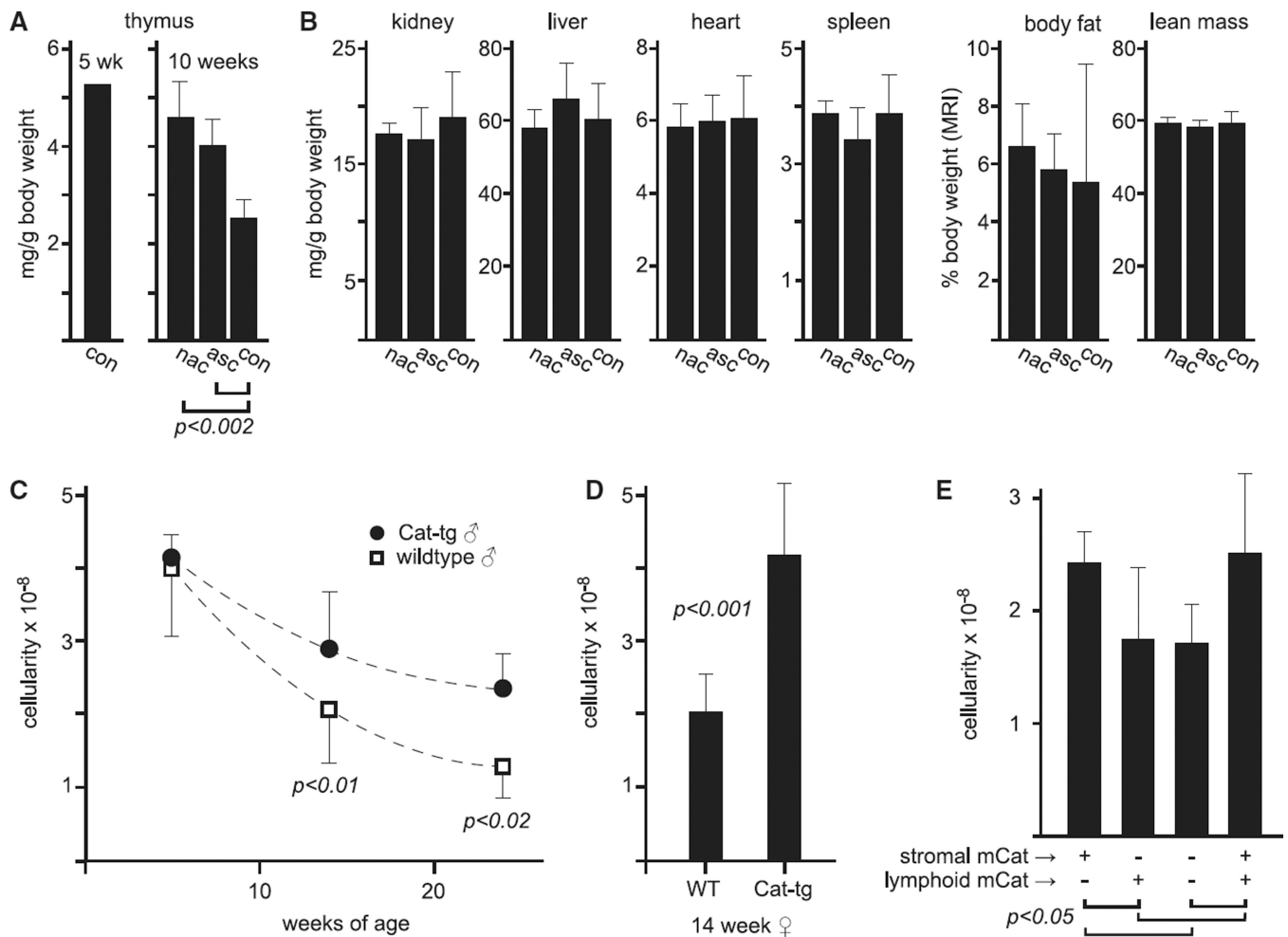


### Figure 3. Thymic Atrophy Is Responsive to Redox State in a Stromal-Dependent Manner

(A) Drinking water containing the antioxidants N-acetylcysteine (nac) or L-ascorbic acid (asc) was given from weaning; thymus weight was measured at 10 weeks. Mice supplemented with antioxidant compounds exhibited significantly larger thymuses than WT control (values indicate mean  $\pm$  SD for five animals, except for young control thymus, which represents a historical average).

(B) No significant differences were found in other organs (kidney, heart, liver, spleen) by weight or in total body fat or lean body mass by MRI.

(C) Thymus cellularity in male mice expressing a catalase transgene (mCatTg) at approximately 1, 3, or 6 months of age. Control and mCatTg thymuses were indistinguishable at 5 weeks of age (i.e., at the peak of thymus size, before the onset of metabolic damage), but while control thymuses subsequently exhibited profound atrophy, mCatTg remained substantially larger and atrophied at a much slower rate. Values indicate the mean  $\pm$  SD for 3–17 animals per time point for each genotype.

(D) Genetic replacement of catalase in female mice has similar effects to males on the inhibition of thymic atrophy. Values represent mean  $\pm$  SD for five (WT) or ten (mCat-tg<sup>+</sup>) mice.

(E) thymus cellularity 10 weeks after reciprocal transplantation of mCatTg or control bone marrow into recipient mice with or without mCatTg; genetic complementation in stromal (recipient) cells was sufficient to achieve full protective effect, while expression in lymphoid (donor) cells had little effect (mean  $\pm$  SD for seven to nine animals). Significance indicates Student's two-tailed t test, independent samples.

Author Manuscript

Author Manuscript

Author Manuscript

Author Manuscript

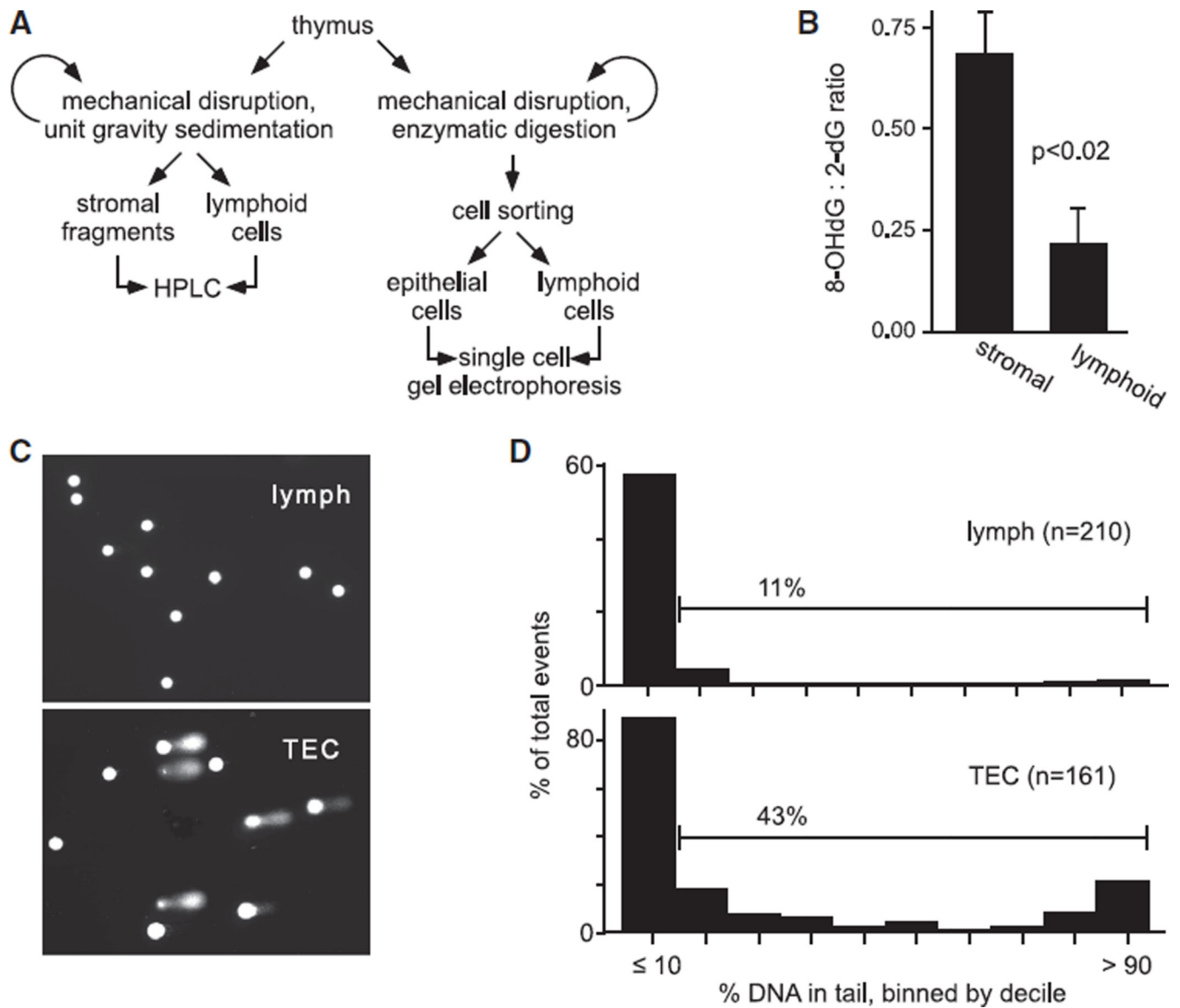


**Figure 4. Thymic Stromal Cells Exhibit Elevated Levels of the Classical Hallmarks of Oxidative Damage**

(A) The experimental approach in brief. Gross enrichment of lymphoid-depleted stromal rudiments was used for HPLC, which required large sample amounts, while SSGE was used highly purified thymic epithelial cells.

(B) The relative abundance of 8OHdG, a product of DNA oxidation, was much higher in stromal samples than in lymphoid cells from the same biological sample ( $n = 3$ ; Student's two-tailed t test, independent samples).

(C) Representative images of SSGE from epithelial or lymphoid cells isolated from the same cell suspension.

(D) Pooled quantitative results of DNA in the “comet” tail, a relative assessment of DNA damage ( $n = 3$ ). For simplicity, data are binned into deciles; significance ( $p < 0.001$ ) indicates the Mann-Whitney U test.

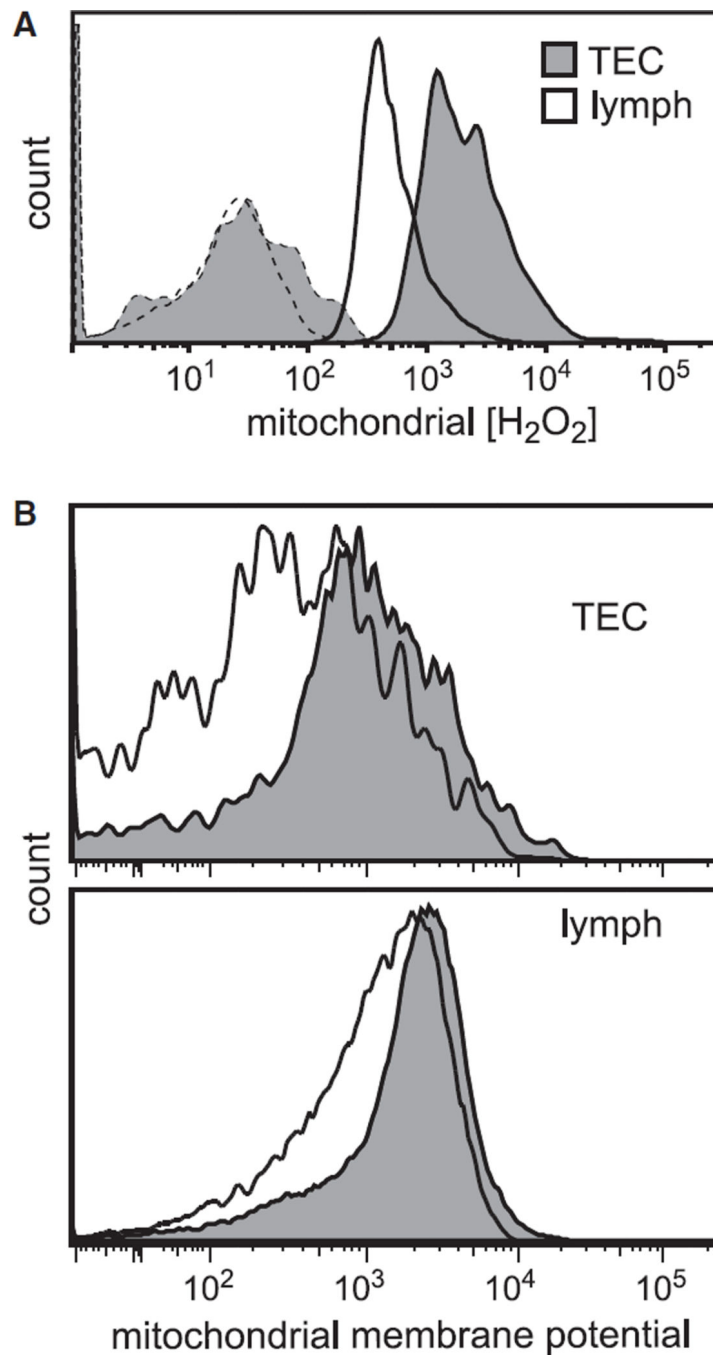


**Figure 5. Epithelial Stromal Cells Accumulate More  $H_2O_2$  and Are More Sensitive to  $H_2O_2$  Damage Than Their Lymphoid Counterparts in the Thymus**

(A) Quantitative measurement of mitochondrial  $H_2O_2$  in TEC versus lymphoid cells from the same cell suspension. Dashed lines indicate background fluorescence in unstained control cells (i.e., no MitoPy1).  $H_2O_2$  concentrations are markedly higher in TEC than in lymphoid cells.

(B) Mitochondrial integrity in gated epithelial or lymphoid cells in the same sample, before (filled histogram) or after (open histogram) a 45-min treatment with 500  $\mu M$   $H_2O_2$ .

Lymphoid cells were relatively unperturbed by H<sub>2</sub>O<sub>2</sub> treatment, while epithelial cells exhibited a more pronounced sensitivity to ROS.

Author Manuscript

Author Manuscript

Author Manuscript

Author Manuscript